Published in final edited form as:

J Mol Biol. 2015 April 24; 427(8): 1765–1778. doi:10.1016/j.jmb.2014.12.004.

Uncovering the role of Sgf73 in maintaining SAGA Deubiquitinating Module Structure and Activity

Ming Yan and Cynthia Wolberger

Department of Biophysics and Biophysical Chemistry, The Johns Hopkins University School of Medicine, 725 N. Wolfe Street, Baltimore, MD 21205, USA

Abstract

The SAGA (Spt-Ada-Gcn5-acetyltransferase) complex performs multiple functions in transcription activation including deubiquitinating histone H2B, which is mediated by a subcomplex called the deubiquitinating module (DUBm). The yeast DUBm comprises a catalytic subunit, Ubp8, and three additional subunits, Sgf11, Sus1 and Sgf73, all of which are required for DUBm activity. A portion of the non-globular Sgf73 subunit lies between the Ubp8 catalytic domain and the ZnF-UBP domain and has been proposed to contribute to deubiquitinating activity by maintaining the catalytic domain in an active conformation. We report structural and solution studies of the DUBm containing two different Sgf73 point mutations that disrupt deubiquitinating activity. We find that the Sgf73 mutations abrogate deubiquitinating activity by impacting the Ubp8 ubiquitin-binding fingers region and have an unexpected effect on the overall folding and stability of the DUBm complex. Taken together, our data suggest a role for Sgf73 in maintaining both the organization and ubiquitin-binding conformation of Ubp8, thereby contributing to overall DUBm activity.

Keywords

Sgf73; SAGA; Ubp8; deubiquitinating enzyme; transcription activation

Introduction

The initiation of transcription in eukaryotes is regulated by coactivators that are recruited to promoters by gene-specific activators [1]. Transcriptional coactivators are typically multisubunit protein complexes that carry out diverse functions including histone modification

Conflict of interest statement

All authors declare that there is no conflict of interest.

Accession Numbers

The coordinates and structure factors for DUBm-Sgf73 $^{\rm Y57A}$ and DUBm-Sgf73 $^{\rm N59D}$ were deposited with the Protein Data Bank under accession numbers **4W4U** and **4WA6** respectively.

Publisher's Disclaimer: This is a PDF file of an unedited manuscript that has been accepted for publication. As a service to our customers we are providing this early version of the manuscript. The manuscript will undergo copyediting, typesetting, and review of the resulting proof before it is published in its final citable form. Please note that during the production process errors may be discovered which could affect the content, and all legal disclaimers that apply to the journal pertain.

^{© 2014} Published by Elsevier Ltd.

^{*}Corresponding author: Cynthia Wolberger, cwolberg@jhmi.edu.

and assembly of the transcription preinitiation complex. The SAGA (Spt-Ada-Gcn5 acetyltransferase) complex is a transcriptional coactivator that is functionally and structurally conserved from yeast to mammals [2] and has been a paradigm for studies of eukaryotic gene activation. SAGA has two enzymatic activities that are crucial for its ability to activate transcription: histone acetylation and deubiquitination of histone H2B [2, 3]. The yeast SAGA complex has a mass of 1.8 MDa and contains 19 proteins that are arranged in a modular fashion into discrete subcomplexes [4, 5]. The histone acetyltransferase (HAT) activity resides in a subcomplex containing the catalytic subunit, Gcn5, along with Ada2, Ada3 and Sgf29 [4]. The deubiquitinating activity of SAGA residues in a distinct subcomplex called the deubiquitinating module (DUBm), which contains the ubiquitinspecific protease, Ubp8, and three additional subunits, Sus1, Sgf11 and Sgf73 [6-9]. H2B monoubiquitination serves as a transient signal during transcription initiation [6, 10]. Monoubiquitination of H2B at Lys123 in yeast is catalyzed by the E2/E3 pair, Rad6/Bre1 [11, 12], which triggers recruitment of the Set1-containing COMPASS complex [12]. Set1 can either di- or trimethylate histone H3 at Lys4 [13, 14], which is a prerequisite for engaging SAGA [14]. In later steps of transcription activation, the removal of ubiquitin from H2B-Lys123 by the SAGA DUBm facilitates recruitment of the Ctk1 kinase and phosphorylation within the Pol II CTD [6, 15]. This phosphorylation is crucial for the transition from transcription initiation to elongation.

The catalytic subunit of the yeast SAGA DUBm, Ubp8, belongs to the ubiquitin-specific protease (USP) family of deubiquitinating enzymes (DUBs) [6, 16, 17]. Although it contains a canonical USP domain, Ubp8 is inactive on its own [17]. Ubp8 only becomes active when it is incorporated into the larger DUBm complex together with Sgf11, Sgf73 and Sus1 [8, 9, 17]. Crystal structures of the SAGA DUBm [18, 19] revealed a highly intertwined organization for Ubp8, Sus1, Sgf11 and Sgf73 in which each subunit contacts the other three (Fig. 1A). Remarkably, only Ubp8 contains globular domains while the other three subunits adopt extended conformations. The DUBm complex is organized into two functional lobes: the ZnF-UBP (assembly) lobe, organized around the Ubp8 ZnF-UBP domain, and the USP (catalytic) lobe, organized around the USP domain of Ubp8 [18, 19]. In the ZnF-UBP lobe, the N-terminal helix of Sgf11 serves as the central organizing unit that is sandwiched between the Ubp8 ZnF-UBP domain and Sus1 (Fig. 1A). The rest of Sgf11, comprising an ordered linker region and a C-terminal zinc finger (ZnF) domain, spans the two lobes and caps off the USP domain of Ubp8, and binds near the active site in the USP lobe (Fig. 1A). The N-terminal portion of Sgf73 (~100 residues) that is incorporated into the DUBm is largely non-globular and is in part sandwiched between the two lobes of the DUBm.

Deletions in both Sgf11 and Sgf73 have particularly dramatic effects in reducing or abrogating DUBm deubiquitinating activity [8, 18]. Deletion of the Sgf11 ZnF results in almost complete loss of Ubp8 catalytic activity [18]. Structural and biophysical studies have shown that removal of the Sgf11 ZnF domain destabilizes the compact folding of the DUBm, leading to formation of a domain-swapped DUBm dimer in which a key active site residue is displaced [20]. Sgf73 is the largest subunit of the DUBm and contains 657 residues, of which the first 96 residues are sufficient for full activity and for incorporation of Sgf73 into the DUB module [8, 18, 19]. The N-terminal residues of Sgf73 wrap around the surface of the ZnF-UBP lobe, while the remainder of the Sgf73 fragment in the crystal is

sandwiched in the cleft between the ZnF-UBP lobe and USP lobe (Fig. 1A) [18, 19]. At the C-terminus of the Sgf73 fragment in the DUB module is a zinc finger (ZnF) whose integrity is essential for the incorporation of this subunit into DUBm as well as for the catalytic activity of Ubp8, as either a short deletion or point mutations in Sgf73 zinc-coordinating residues disrupt the association of Sgf73 with the rest of the DUBm [18].

The underlying mechanism by which Sgf73 maintains the catalytic activity of DUBm has remained elusive. One hypothesis [19] is that Sgf73 promotes ubiquitin binding by maintaining the fingers domain of Ubp8 in a conformation capable of binding ubiquitin. In the presence of Sgf73, the fingers domain of Ubp8 remains in an "open" conformation, even in the absence of bound ubiquitin [19]. By contrast, the same region of the human USP8 Apo protein collapses inward and occludes the ubiquitin-binding pocket (Fig. 1B) [21]. It has also been suggested that Sgf73 contributes to DUBm activity by maintaining the overall organization of the DUBm [18], including the relative positions of the two lobes of the complex and the conformation of the linker connecting the two Ubp8 domains. We report here structural and functional studies aimed at determining the role that Sgf73 plays in maintaining the deubiquitinating activity of the SAGA DUB module. We engineered two point mutations that were predicted to disrupt the ability of Sgf73 to maintain the open conformation of the Ubp8 ubiquitin-binding pocket and show that these mutations disrupt the enzymatic activity of the DUBm. Crystal structures of the DUBm containing the Sgf73 point mutants reveal perturbations in the ubiquitin-binding region of Ubp8 that affects substrate ubiquitin binding. We unexpectedly found that the Sgf73 point mutations destabilize the overall thermal stability of DUBm complex, thereby impacting both the enzymatic activity of the DUBm as well as ubiquitin binding. Together, these results suggest a role for Sgf73 in regulating Ubp8 activity by both maintaining the overall structure of ubiquitin-binding pocket of Ubp8 as well as the stability and folding of the DUBm.

Results

Sgf73 point mutants that abrogate the enzymatic activity of the DUB module

The extensive interactions between Sgf73 and the catalytic domain of Ubp8 have led to speculation that these interactions directly impact Ubp8 deubiquitinating activity through structural or allosteric mechanisms [18,19]. The catalytic domain of USP family DUBs can be divided into three sub-domains: Fingers, Palm, and Thumb [22]. The curved fingers domain presents a large surface pocket, which is expected to accommodate the globular domain of ubiquitin with support from the other two sub-domains. In both the apo-enzyme (DUBm-apo) [18, 19] and the structure of the DUBm bound to ubiquitin aldehyde (DUBm-Ubal) [19], the fingers domain of Ubp8 is in the same "open" conformation that accommodates ubiquitin (Fig. 1A). This observation led to the speculation that, in contrast with some other USP DUBs that must undergo a conformational change to accommodate the ubiquitin substrate [21,23], Sgf73 helps to maintain Ubp8 in a conformation that is competent for ubiquitin binding.

We inspected the interface between Ubp8 and Sgf73 to look for residues that are in a position to maintain the conformation of the fingers domain irrespective of whether or not ubiquitin is bound. In the DUBm structure, the Sgf73 H3-L3 region (Fig. 1A) contacts the

"back" side of the Ubp8 fingers domain, distal from the ubiquitin binding surface, placing it in a position to influence the structure of the ubiquitin-binding region. Sgf73 residues Tyr57, Asn59 and Asn61 form a set of hydrophobic and hydrogen-binding interactions with the fingers domain of Ubp8 and could thus potentially affect ubiquitin binding (Fig. 1C). We introduced point mutations at these positions and assayed the activity of the mutant DUBm complexes using the model DUB substrate, ubiquitin-AMC [24]. We found that mutation of Tyr57, a residue that is buried in a hydrophobic pocket formed by a group of residues on the "back" side of the Ubp8 fingers domain (Fig. 1C), abolished the catalytic activity of Ubp8 (Fig. 2A). Mutations at Asn59 or Asn61, which form multiple hydrogen bonds and charge-charge interactions with Ubp8 (Fig. 1C), have a more moderate effect in decreasing the catalytic activity of the DUB module (Fig. 2A).

Previous work had found that the integrity of the Sgf73 zinc finger, which is wedged between the two globular domains of Ubp8 and is partly solvent-exposed (Fig. 1D), is critical for DUBm activity [18, 19]. Both deletions and mutations in the Sgf73 zinc-chelating residues were shown to disrupt both the integrity and catalytic activity of the DUBm [18, 19], although these studies did not address the contribution to catalytic activity of zinc finger residues that contact Ubp8. Sgf73 zinc finger residues Glu79 and Lys83 each lie at the surface of the DUBm and form bridging contacts with Ubp8 (Fig. 1D). Substitution of either of these residues with alanine, however, did not have a significant effect on Ub-AMC hydrolysis as compared to the wild type DUBm (Fig. 2A).

To verify that the observed effects of Sgf73 mutants were not substrate-specific, DUBm activity was assayed using K48-linked diubiquitin, which can also be cleaved by the DUBm [20]. As shown in Figure 2B, the effects of Sgf73 mutations Y57A, N59D and E79A on DUBm cleavage of K48-linked diubiquitin substrate are comparable to those observed in ubiquitin-AMC hydrolysis assays (Fig. 2A). Overall, these data suggest that the H3-L3 region of Sgf73 plays an essential role in priming Ubp8 for activity.

Crystal structures of Sgf73 mutants

To gain insight into the role of the Sgf73 H3-L3 region in regulating the catalytic activity of Ubp8, we crystallized the DUBm complex containing either the Sgf73 Y57A or Sgf73 N59D point substitution in the N-terminal Sgf73 fragment, Sgf73 1-96. Unlike the apo DUBm or DUBm bound to ubiquitin aldehyde (Ubal), all of which crystallize with only one complex in the asymmetric unit [18, 19], both mutant complexes crystallized with two complexes in the asymmetric unit of space group P2₁ (Fig. S2A). The structures of DUBm-Sgf73 Y57A and DUBm-Sgf73 N59D were determined at 2.8 Å and 2.4 Å resolution, respectively (data collection and refinement statistics are given in Table 1). While the overall architecture of the DUBm-Sgf73 Y57A or DUBm-Sgf73 Complex is similar to that observed in previously determined wild type structures (Fig. S1), we note that the Sgf11 zinc finger is either partially (DUBm-Sgf73 N59D) or completely (DUBm-Sgf73 Y57A) disordered in Sgf73 mutant structures (Figs. S3A and S3B). This was unexpected because the Sgf11 zinc finger is not near the Sgf73 point mutation sites, nor is there any evident perturbation in the Ubp8 structure in the vicinity of the binding site for the Sgf11 zinc finger. The connection between the Sgf73 mutations and disorder of the Sgf11 zinc finger remains unclear. In addition, in

both structures of the apo DUB module containing Sgf73^{Y57A} or Sgf73^{N59D} (Fig. S1), the fingers domain is well-ordered in one complex (Figs. S4A and S4B) in the asymmetric unit while the distal, zinc-binding portion of the Ubp8 fingers domain is partially disordered in the second complex (Fig. S2A). In previously reported structures of the DUBm in the absence of bound ubiquitin, the zinc-binding tip of the fingers domains is also partially disordered [18, 19], whereas these residues are ordered in the structure of the DUBm-Ubal complex [19].

A comparison of the mutant and wild type DUBm structures reveals differences in the beta sheet portions of the ubiquitin-binding fingers region in both the DUBm-Sgf73^{Y57A} and DUBm-Sgf73^{N59D} structures. In both copies of the DUBm in the asymmetric unit, there is an inward movement of the Ubp8 beta sheet towards the ubiquitin-binding pocket, with beta strand 7 showing the most significant movement of up to 3.2 Å towards the ubiquitin-binding region (Fig. 3A). This conformational change is seen in both complexes in the asymmetric unit (Figs. 3A, S2B and S2C) and in both Sgf73 mutant complexes (data now shown). In addition, the distal tip of the Ubp8 fingers domain, which is well-ordered in one of the complexes in the asymmetric unit (Figs. S4A and S4B), has moved up to 5.0 Å toward the ubiquitin-binding pocket, further occluding the ubiquitin-binding site (Fig. 3A). The conformational changes in both beta strand 7 and the finger tip region of Ubp8 have the potential to negatively impact ubiquitin binding as a result of steric clashes between Ubp8 and the bound ubiquitin (Fig. 3B).

To investigate whether the Sgf73 mutations induce conformational changes in the Ubp8 fingers domain, we analyzed the structural rearrangements in the vicinity of the Sgf73 mutation sites. The Sgf73-Y57A substitution abolishes the hydrophobic interactions between the Sgf73 H3-L3 region and Ubp8 fingers domain (Fig. 4A). Without the interactions mediated by Tyr57, the side chain of Lys56 is re-orientated and the hydrophobic patches on the backside of the Ubp8 fingers domain are completely exposed (Fig. 4A). In the DUBm-Sgf73^{N59D} structure, replacement of Asn59 with Asp59 disrupts the hydrogen-binding interactions between Asn59 and Leu354, Glu280 of Ubp8 (Fig. 4B). Additionally, the re-oriented Asp59 leads to dislocation of the side chain of Asn61, which further disrupts the interactions between Asn61 and Cys271, Glu272 of Ubp8 (Fig. 4B). Nonetheless, it is not immediately obvious how these structural differences are transmitted to the distal portion of Ubp8 fingers domain.

We considered the possible role of crystal contacts in governing the observed changes in the Ubp8 fingers domain in the presence of Sgf73 mutants. Both mutant DUB modules crystallize with a packing arrangement that differs from the wild type [19]. The crystal contacts with the Ubp8 fingers domain are thus different in the wild type and mutant DUBm crystals, although both crystal lattices have contacts with the Ubp8 fingers domain (Fig. S5). We were unable to crystallize the mutant DUBm-Sgf73^{Y57A} and DUBm-Sgf73^{N59D} complexes in the same crystallization conditions that yielded the wild type crystals [19], nor could we crystallize the wild type DUBm in the same conditions as the mutant DUB module, suggesting that intrinsic differences in the DUBm arising from the Sgf73 point mutations may favor a different packing arrangement than the wild type complex.

The conformational changes in Ubp8 that would be needed to alleviate clashes with bound ubiquitin are predicted to exact an energetic cost that would be reflected in a decreased affinity for ubiquitin. We compared the affinity of K48-linked diubiquitin for either DUBm-WT or DUBm-Sgf73 Y57A using isothermal titration calorimetry (ITC). To prevent hydrolysis of the diubiquitin substrate, the active site cysteine of Ubp8 was mutated to alanine. We found only a modest increase in the dissociation constant, from $0.4\pm0.1\mu M$ at 24 °C for the wild type DUBm (Fig. 7A, Table 2) to $0.67\pm0.04\mu M$ for the mutant DUBm-Sgf73 Y57A (Fig. 7C, Table 2). This modest decrease in affinity does not account for the magnitude of the decrease in DUBm ubiquitin hydrolase activity in the presence of the Sgf73-Y57A mutation (Figs. 2A and 2B), suggesting that additional features of the mutant complex must also contribute to the decrease in enzymatic activity.

Sgf73 point mutations reduce the stability of the DUB module

While structures of the DUBm containing Sgf73 point mutations Y57A or N59D reveal some structural rearrangements that could impact Ubp8 deubiquitinating activity (Fig. 3A), they do not account for the magnitude of the observed effect on enzymatic activity (Figs. 2A and 2B). To explore whether there were additional factors that reduced the catalytic activity of the DUBm, we asked whether the overall stability of the complex was affected by either Sgf73 point mutation. The overall stability of the four-protein DUBm was assayed using the thermal shift (ThermoFluor) assay [25], in which an environmentally sensitive fluorescent dye is used to monitor protein unfolding as a function of increasing temperature. An initial experiment was performed with the fluorescent dye, Sypro Orange (Fig. 5A), which has a low quantum yield in aqueous solution but is highly fluorescent in nonpolar environments with low dielectric constants such as hydrophobic sites in proteins. When a protein starts to unfold, the dye binds to exposed hydrophobic regions of the protein, resulting in an increase in fluorescence emission. The fluorescence intensity reaches a maximum and then starts to decrease, most likely due to precipitation of the proteins along with the fluorescent probe. As shown in Figure 5A, the wild type DUBm has a melting temperature (T_m) of 55 °C, whereas the DUBm containing the Sgf73 Y57A and N59D mutations decrease the DUBm melting temperature to 34 °C and 44 °C, respectively. By contrast, the mutation Sgf73 E79A, which is solvent-exposed and is not expected to affect complex folding, has no effect on the T_m (Fig. 5B).

To investigate whether the reduced thermal stability of DUBm-Sgf73^{Y57A} or DUBm-Sgf73^{N59D} was due to the disorder of Sgf11 ZnF domain that was observed in those mutants (Figs. S3A and S3B), we also assayed the melting temperature of DUBm containing wild type Sgf73 but lacking the Sgf11 ZnF domain (DUBm-Sgf11 ^{Znf}) (Fig. S6). The results suggest that the disorder of Sgf11 ZnF does not impact the overall thermal stability of the complex. We speculate that the higher basal fluorescence intensities observed at low temperatures for both DUBm-Sgf73^{Y57A} and DUBm-Sgf73^{N59D} mutant complexes may be due to exposure of hydrophobic dye-binding interfaces between the Sgf73 H3-L3 region and the backside of the Ubp8 fingers domain (Fig. 1C). Alternatively, the destabilizing effect of these mutations may simply enable more "breathing" of the DUBm, with transient conformational changes that further expose the hydrophobic subunit interfaces to solvent and thus dye binding.

The decrease in T_m indicates that both Sgf73 interface mutations significantly reduce the overall stability of the DUBm. The effect is greater in the case of the Sgf73-Y57A substitution, which disrupts the hydrophobic interactions between Sgf73 and the backside of Ubp8 fingers domain that is essential to the molecular interface joining two lobes of the DUB module (Fig. 4A). Since both mutant DUB modules were crystallized at 20° C, which is well below either melting temperature, the complexes were sufficiently well-folded to form stable packing interactions. However, the enzymatic assays were carried out at 30° C, which is just below the Tm of the DUBm-Sgf73^{Y57A} complex and is thus in a range in which the mutant DUBm might be expected to be destabilized and potentially inactivated.

The enzymatic activity of DUBm-Sgf73^{Y57A} is temperature sensitive

To investigate whether the observed effects of Sgf73 mutations on DUB module stability account for the decrease in enzymatic activity, we assayed the deubiquitinating activity of wild type and mutant DUB modules at different temperatures. Cleavage of fluoresceinlabeled K48 diubiquitin was assayed at temperatures ranging from 10 to 35°C (Fig. 6A). The peak in wild type DUBm activity is between 25°C – 30°C and changes little at 35°C (Fig. 6A). By contrast, the overall activity of the DUBm-Sgf73^{Y57A} mutant is lower than the wild type over all temperatures assayed. Importantly, the activity starts to decrease at 25°C and is significantly reduced at 30°C. At 35°C, the enzymatic activity of DUBm-Sgf73^{Y57A} is almost undetectable (Fig. 6A). Activity could not be monitored at temperatures higher than 35°C, as the DUBm-Sgf73^{Y57A} started to precipitate at these temperatures. The overall activity of DUBm-Sgf73^{N59D} was somewhat lower than that of the wild type complex but exhibited only modestly greater temperature sensitivity at 35°C (Figs. 6A and 6B). The behavior of both mutants can therefore be explained at least in part with the impact of Sgf73 mutations on complex stability at the assay temperature and agrees with the results of the thermal shift assays showing a marked destabilization of DUBm-Sgf73Y57A and only modest destabilization of DUBm-Sgf73N59D (Fig. 5B).

To explore whether the structural changes at higher temperature were reversible, we incubated DUBm-Sgf73^{Y57A} at 35°C for 10 minutes, then shifted the temperature to 20°C and assayed cleavage of K48-linked diubiquitin (Fig. 6C). Whereas this mutant complex has negligible activity at 35°C (Fig. 6A Lane 13), the activity is restored when the temperature is shifted back to 20°C (Fig. 6D). These results indicate that whatever conformational changes occur at higher temperature are reversible within the temperature range that we performed the experiments.

The point mutation, Y57A, which disrupts hydrophobic interactions between the H3-L3 region of Sgf73 and the fingers domain of Ubp8 (Fig. 4A), gives rise to modest conformational changes confined to the fingers domain of Ubp8 in the crystal structure (Fig. 3A), which was grown at 20°C. We speculated that the greater thermal motions of the protein subunits at elevated temperatures have the potential to disrupt Sgf73 H3-L3 interactions with Ubp8, and that this effect may be magnified by the Sgf73 point mutations, which lie at this interface (Figs. 4A and 4B). Without the wild type network of contacts between Sgf73 and the backside of the Ubp8 fingers domain, the fingers domain may collapse inward and impede ubiquitin binding. To test this hypothesis, we measured the

affinity of the mutant DUBm-Ubp8^{C146A}-Sgf73^{Y57A} complex, containing both the mutant Sgf73 protein and catalytically inactive Ubp8, for K48-linked diubiquitin at different temperatures using isothermal titration calorimetry (ITC) (Figs. 7B-F). The same amount of DUBm-Ubp8^{C146A}-Sgf73^{Y57A} and K48-linked diubiquitin were used in ITC experiments at temperatures ranging from 20°C to 35°C. The ITC data neared complete saturation and were fit by a single-site model except for the experiment performed at 35°C, which could not be fit to any model, most likely due to sample aggregation and precipitation. At 20°C (Fig. 7B, Table 2), DUBm-Ubp8^{C146A}-Sgf73^{Y57A} bound to K48-linked diubiquitin with a K_d 20°C of 0.4 µM, which is comparable to the affinity for diubiquitin of the DUBm with wild type Sgf73 (DUBm-Ubp8^{C146A}) measured at 24°C (Fig. 7A, Table 2). The affinity of the DUBm containing the Sgf73-Y57A mutation decreases as the temperature is raised, reaching a K_d value of 1.2 µM at 28°C and 6.7 µM at 32°C. In addition, the N value, which represents binding stoichiometry, decreases from a value of 0.7 in binding experiments conducted between 20°C and 28°C to 0.4 at 32°C. The lower N value suggests that a decreased proportion of the total complex in the sample cell is competent for ligand binding, as might occur as a higher proportion of DUBm complexes shift to a partially dissociated or unfolded state.

Taken together, these data point to a correlation between complex conformation and catalytic activity of the DUBm. At lower temperatures, the mutants adopt a conformation that more closely resembles the wild type DUBm and the catalytic activity is largely, though not completely, preserved. As the temperature increases, we speculate that the detachment of Sgf73 H3-L3 region from the backside of Ubp8 leads to rearrangement of the ubiquitin-binding region. The "closed" binding pocket impedes ubiquitin binding and results in a decrease in catalytic activity. Once the temperature is lowered, the interactions between Sgf73 H3-L3 region and Ubp8 are restored and ubiquitin-binding pocket is reorganized into the "open" conformation. Furthermore, these data suggest a primary role for Sgf73 in DUBm activation by maintaining the overall architecture of the complex, especially the conformation of Ubp8 ubiquitin-binding region.

Discussion

An increasing number of studies have demonstrated that protein partners dictate the enzymatic activities of many deubiquitinating enzymes [26, 27]. For example, USP14, UCH37 and Rpn11 are active once they are associated with proteasome [28–31]. USP1, USP12 and USP46 all require the regulatory protein UAF1 for activity [32–34] and BAP1 requires ASX in order to deubiquitinate histone H2A [35]. In addition, the C-terminal ubiquitin-like domain of USP7/HAUSP can activate its own enzymatic activity, with the activation enhanced allosterically by GMP-synthetase [23]. However, the mechanisms by which the partner proteins modulate the activities of these DUBs are still poorly understood. In the yeast SAGA DUB module, the activity of the deubiquitinating enzyme, Ubp8, is orchestrated by three other subunits – Sgf73, Sgf11 and Sus1 – which are required for full enzymatic activity [8, 9, 17]. The location of Sgf73, which is sandwiched between the Ubp8 catalytic domain and the ZnF-UBP lobe of the DUB module (Fig. 1A), and the deleterious effects of deletions within this portion of Sgf73 [18] pointed to a role for Sgf73 in organizing the two lobes of the DUB module. In addition, structural comparisons between

Ubp8 and other DUBs such as hUSP8 [21] suggested a potential role for Sgf73 in maintaining a conformation of the Ubp8 ubiquitin binding region that is competent to bind ubiquitin, thereby prepaying the energetic cost of induced conformational changes. In this study, we mutated residues in Sgf73 that were predicted to disrupt the packing of the Sgf73 H3-L3 region against the backside of the Ubp8 fingers domain and thereby perturb the structure of the ubiquitin-binding pocket and interfere with ubiquitin binding. We found that Sgf73 Y57A and N59D mutations within the H3-L3 region significantly reduced the catalytic activity of the DUBm (Figs. 2A and 2B). Crystal structures of the mutant complexes revealed modest changes in the Ubp8 fingers region that could interfere with ubiquitin binding (Fig. 3A). However, binding studies (Figs. 6A and 6C) indicated that the effects of the mutations on substrate ubiquitin binding could not fully account for the effects of the mutations in enzymatic assays, which were conducted at 30°C. Instead, we found that the Sgf73 mutations reduced the overall stability of the DUB module, as reflected in a lowered melting temperature (Fig. 5A) and higher enzymatic activity at lower temperatures (10°C – 20°C) (Figs. 6A and 6B). Enzymatic activity decreased as the temperature increased from 20°C to 35°C (Figs. 6A and 6B), consistent with destabilization of the DUBm. The decrease in activity with increasing temperature was most dramatic for the Sgf73-Y57A mutation, which disrupts a significant number of hydrophobic interactions between Sgf73 and Ubp8 (Fig. 4A). These results reveal to an unexpected sensitivity of DUB module stability to even small perturbations, further highlighting the absolute dependence of Ubp8 activity on its proper incorporation into the DUB module.

Our biophysical studies of the Sgf73 point mutations, combined with previous studies of the role of the Sgf11 subunit in DUB module activity [18, 20] suggest a model for how destabilization of Sgf73 binding to Ubp8 leads to marked decreases in enzymatic activity. Sgf73 is the least stably incorporated DUBm subunit as judged by how readily Sgf73 can be separated from the other three subunits in the presence of EDTA [19]. At elevated temperatures, we speculate that the H3-L3 region of Sgf73 (Fig. 1A) is dislodged from the "back" side of the Ubp8 fingers domain and becomes mobile or disordered. Without the support of Sgf73, the ubiquitin-binding pocket of Ubp8 may further collapse and thus have decreased affinity for ubiquitin. In addition, the two lobes of the DUBm could separate, which would impact the position of the critical catalytic residue, N141, located in Ubp8 loop L2 that connects the two globular domains of Ubp8 (Fig. S7). This conserved USP domain residue stabilizes the oxyanion intermediate in the isopeptidase reaction [22]. The conformation of loop L2 depends upon the compact wild type conformation of the DUB module, which is stabilized by the Sgf11 zinc finger (Fig. S7). When the Sgf11 zinc finger is deleted, the USP and ZnF-UBP lobes of the DUBm separate, displacing loop L2 of Ubp8 and thus removing the oxyanion stabilizing residue, N141, from the vicinity of the active site [20]. The destabilized DUBm can associate with a second dissociated complex to form a domain-swapped dimer of DUB modules in which loop L2 is displaced and N141 is thus far from the Ubp8 active site [20]. The DUB modules containing Sgf73 mutants in present study had unanticipated disorder in the Sgf11 zinc finger, particularly in the presence of the Sgf73-Y57A mutation (Figs. S1 and S3A). Further studies will be needed to elucidate how the Sgf73 mutations impact the Sgf11 zinc finger given the large distance separating these regions and the absence of local rearrangements in Ubp8 or changes in crystal packing that

might influence Sgf11 zinc finger structure or binding to Ubp8. Since Sgf11 helps to stabilize the position of Ubp8 loop L2, any decrease in the binding of Sgf11 to Ubp8 could lead to an increase in mobility of loop L2 and thereby displace the critical N141 residue. Thus, besides performing an essential role in DUBm activation by stabilizing the ubiquitin binding pocket and promoting the substrate binding, Sgf73 could also regulate the enzymatic activity of DUBm by maintaining the "competent" state of the Ubp8 catalytic center.

The observed sensitivity of DUB module activity and folding to mutations and deletions in Sgf73, as well as in the other subunits, suggests possible avenues for developing novel cancer therapies targeting USP22, the human homologue of Ubp8. USP22 is a subunit of the TFTC/STAGA and human SAGA transcriptional coactivator complexes [36,37] and, like yeast Ubp8, must be incorporated into the human DUB module for full activity [38]. USP22 is overexpressed in a variety of tumors [36,37,39] and is a marker for malignancies that respond poorly to chemotherapy [40,41]. These tumors also have decreased levels of H2B ubiquitination [42,43], indicating a connection between USP22, human DUBm activity and tumor growth. Identifying drugs that target specific deubiquitinating enzymes has been a challenge because of the more than 50 members of the USP family in the human genome and the similarity of their active sites [44]. Our findings suggest a promising alternative strategy for identifying small molecules that could intercalate between ATAXIN-7, the Sgf73 homologue, and USP22 and thus destabilize overall DUB module folding. Screening for molecules that destabilize human DUBm folding using the Thermafluor assay [25] could thus provide a rapid means for identifying candidates for further characterization in enzymatic and cell-based assays. Molecules that specifically target the association of USP22 with the other human DUBm subunits have the potential to be highly specific inhibitors of USP22, and thus promising therapies against tumors that are resistant to current treatments.

Materials and Methods

Cloning, protein expression and purification

Rosetta 2(DE3) pLysS cells (EMD Millipore, Merck KGaA, Darmstadt, Germany) were transformed with three plasmids encoding (1) Ubp8^{WT}, or Ubp8^{C146A} (pET-32a, EMD Millipore), (2) Sus1 (pRSF-1, EMD Millipore), and (3) Sgf73^{WT(1-96)}, Sgf73^{Y57A(1-96)}, Sgf73^{N59D(1-96)}, Sgf73^{N61D(1-96)}, Sgf73^{E79A(1-96)}, or Sgf73^{K83A(1-96)} (pCDFDuet-1 MCSII, EMD Millipore), which was cloned into the same vector as Sgf11^{WT} (pCDFDuet-1 MCSI, EMD Millipore). All versions of the DUBm complex were co-expressed and purified using the previously reported protocol for the expression and purification of wild-type DUBm [19].

Protein crystallization

Crystals were grown by the hanging drop method in VDXm24 plates with sealant (Hampton Research, Aliso Viejo, CA). DUBm-Sgf73^{Y57A} and DUBm-Sgf73^{N59D} crystals grew in 0.1M Bis-Tris pH5.5, 18% PEG3350, 0.1M Ammonium Sulfate using a 1:1 ratio of protein to well solution. Crystals formed grew to a size of ~20 \times 20 \times 300 μm within 3 days at 18°C and were flash-frozen in liquid nitrogen in the presence of mother liquor supplemented with 20% ethylene glycol as a cryo-protectant.

Date collection, structure determination and refinement

X-ray diffraction data from DUBm-Sgf73^{Y57A} and DUBm-Sgf73^{N59D} crystals were collected at GM/CA CAT beamline 23ID-D at the Advanced Photon Source. Crystals that had been frozen in cryo-protectant and stored in pucks were loaded into a sample exchange robot (ALS/Berkeley type) and data were collected on a MarMosiac 300 CCD detector. The structures of both complexes were determined by molecular replacement with Phaser-MR using the coordinates of the wild-type DUBm (PDB ID: 3MHS) as the search model. The DUBm-Sgf73^{Y57A} and DUBm-Sgf73^{N59D} structures were refined with PHENIX [45] and Refmac [46]. Coot [47] was used for manual model building. PyMOL Version 1.5.0.4 (Schrödinger, LLC) was used to generate all structure figures.

Ubiquitin-AMC hydrolysis Assay

Assays were conducted in 384-well black polystyrene micro-plates at 30°C in a POLARstar Omega plate reader (BMG Labtech, Cary, NC) using an excitation wavelength of 385 nm and emission wavelength of 460 nm. Reactions were performed in DUBm assay buffer containing 50 mM HEPES, pH 7.6, 150 mM NaCl, 5uM ZnCl₂, 5 mM dithiothreitol (DTT) and 7.5% DMSO. The wild type DUBm and Sgf73 mutants were held at a concentration of 125 nM. Ubiquitin-AMC (Boston Biochem, Cambridge, MA) was diluted into assay buffer and incubated at 30°C for 10 min inside the plate reader. 3 μ l of recombinant DUBm was also pre-incubated at 30°C for 10 min before mixing with diluted ubiquitin-AMC buffer to a total volume of 30 μ l. The release of AMC was followed at 460 nm, and the first 0–60 s of data were used to fit initial rate.

K48-linked Diubiquitin Cleavage Assay

The concentration of the K48-linked diubiquitin stock was determined by measuring the absorbance at a wavelength of 280 nm using as the extinction coefficient $\varepsilon_{\text{di-Ub}}$ =2980 $M^{-1}\text{cm}^{-1}$. Diubiquitin was diluted with DUBm assay buffer (see above) to yield a final reaction concentration of 5 uM in a reaction volume of 50 µl. A 5 µl volume of enzyme at 5 µM was added at 30°C, and 45 µl of diubiquitin was added and mixed by pipetting 5 times. A 10 µl sample was removed for the 0 min time point and quenched with 5 µl lithium dodecyl sulfate (LDS) buffer. Similar samples were obtained for 5 min., 10 min. and 30 min. A 15 µl aliquot of each sample was loaded into a 4%–12% gradient Bis-Tris NU-PAGE gel (Invitrogen, Grand Island, NY) for SDS-PAGE, and the gels were stained with Coomassie Brilliant Blue.

Thermal Shift Assay

Thermal shift assay curves were collected using an Opticon 2 real-time PCR detector (BioRad) to measure the fluorescence of SYPRO Orange (Molecular Probes) in the presence of wild type DUBm (WT), DUBm-Sgf73^{Y57A}, DUBm-Sgf73^{N59D} and DUBm-Sgf73^{E79A}. Proteins were centrifuged for 30 minutes at 25000g at 4°C before sample preparation. DUBm complex (final concentration at 0.5 mg/ml) and SYPRO Orange dye (diluted 2000 folds to final concentration 2.5X) were mixed in the same buffer as K48-linked cleavage assay and added to 96-well thin-wall PCR plate (Bio-Rad). The temperature was increased

from 5°C to 95°C in increments of 1°C and the fluorescence signals were collected. The wavelengths for excitation and emission were 490 and 575 nm, respectively.

Isothermal Titration Calorimetry (ITC)

ITC measurements were performed by using a Microcal (Amherst, MA) ITC200 calorimeter at either 20°C, 24°C, 28°C, 32°C and 35°C, respectively. DUBm wild type and Sgf73 mutant complexes and K48-linked diubiquitin samples were buffered with 20 mM HEPES, pH 7, 150 mM NaCl, 5 nM ZnCl₂, 0.5 mM Tris (2-Carboxyethyl) phosphine hydrochloride (TCEP) and thoroughly degassed before use. The protein concentrations were determined by amino acid analysis. The sample cell (1.4 ml) contained either 30 μ M DUBm-WT or DUBm Sgf73 mutant. A total of 20 injections of 10 μ l of K48-linked diubiquitin solution (0.3 mM) were carried out at 180 s or 300 s intervals. The heat generated due to dilution of the titrants was subtracted for baseline correction. The baseline-corrected data were analyzed with Microcal ORI-GIN Ver. 7.0 software. All experiments were duplicated.

Supplementary Material

Refer to Web version on PubMed Central for supplementary material.

Acknowledgments

We thank Xiangbin Zhang for generating mutants of Sgf73 and Pankaj Kumar, Anthony DiBello, Alison Ringel and other members of the Wolberger lab for helpful discussions. This work was supported by National Institute of General Medical Sciences grant GM-095822 (C.W.) and by the Howard Hughes Medical Institute. GM/CA @ APS has been funded by the National Cancer Institute (Y1-CO-1020) and the National Institute of General Medical Sciences (Y1-GM-1104). Use of the Advanced Photon Source was supported by the U.S. Department of Energy, Basic Energy Sciences, Office of Science, under contract No. DE-AC02-06CH11357.

Abbreviations

UBP Ubiquitin-specific processing protease

DUB deubiquitinating enzyme

DUBm deubiquitinating enzyme module

Ubal ubiquitin aldehyde

COMPASS Complex Proteins Associated with Set1

CTD C-terminal domain

ubiquitin-AMC Ubiquitin-7-amino-4-methylcoumarin

References

- Weake VM, Workman JL. Inducible gene expression: diverse regulatory mechanisms. Nat Rev Genet. 2010; 11:426–37. [PubMed: 20421872]
- Koutelou E, Hirsch CL, Dent S. Multiple faces of the SAGA complex. Current Opinion in Cell Biology. 2010:22. [PubMed: 21074980]
- Rodriguez-Navarro S. Insights into SAGA function during gene expression. EMBO Rep. 2009; 10:843–50. [PubMed: 19609321]

 Lee KK, Sardiu ME, Swanson SK, Gilmore JM, Torok M, Grant PA, et al. Combinatorial depletion analysis to assemble the network architecture of the SAGA and ADA chromatin remodeling complexes. Mol Syst Biol. 2011; 7:503. [PubMed: 21734642]

- Daniel JA, Grant PA. Multi-tasking on chromatin with the SAGA coactivator complexes. Mutat Res. 2007:618.
- Henry KW, Wyce A, Lo WS, Duggan LJ, Emre NC, Kao CF, et al. Transcriptional activation via sequential histone H2B ubiquitylation and deubiquitylation, mediated by SAGA-associated Ubp8. Genes Dev. 2003; 17:2648–63. [PubMed: 14563679]
- Kohler A, Garcia PP, Llopis A, Zapater M, Posas F, Hurt E, et al. The mRNA export factor Sus1 is involved in Spt:Ada:Gcn5 acetyltransferase-mediated H2B deubiquitinylation through its interaction with Ubp8 and Sgf11. Mol Biol of Cell. 2006:17.
- 8. Kohler A, Schneider M, Cabal GG, Nehrbass U, Hurt E. Yeast Ataxin-7 links histone deubiquitination with gene gating and mRNA export. Nat Cell Biol. 2008; 10:707–15. [PubMed: 18488019]
- Lee KK, Swanson SK, Florens L, Washburn MP, Workman JL. Yeast Sgf73/Ataxin-7 serves to anchor the deubiquitination module into both SAGA and Slik(SALSA) HAT complexes. Epigenetics Chromatin. 2009; 2:2. [PubMed: 19226466]
- Wyce A, Henry KW, Berger SL. H2B ubiquitylation and de-ubiquitylation in gene activation. Novartis Found Symp. 2004; 259:63–73. discussion -7, 163–9. [PubMed: 15171247]
- 11. Robzyk K, Recht J, Osley MA. Rad6-dependent ubiquitination of histone H2B in yeast. Science. 2000; 287:501–4. [PubMed: 10642555]
- Hwang WW, Venkatasubrahmanyam S, Ianculescu AG, Tong A, Boone C, Madhani HD. A conserved RING finger protein required for histone H2B monoubiquitination and cell size control. Mol Cell. 2003:11. [PubMed: 12535517]
- Lee JS, Shukla A, Schneider J, Swanson SK, Washburn MP, Florens L, et al. Histone crosstalk between H2B monoubiquitination and H3 methylation mediated by COMPASS. Cell. 2007; 131:1084–96. [PubMed: 18083099]
- Schneider J, Wood A, Lee JS, Schuster R, Dueker J, Maguire C, et al. Molecular regulation of histone H3 trimethylation by COMPASS and the regulation of gene expression. Mol Cell. 2005; 19:849–56. [PubMed: 16168379]
- Daniel JA, Torok MS, Sun ZW, Schieltz D, Allis CD, Yates JR 3rd, et al. Deubiquitination of histone H2B by a yeast acetyltransferase complex regulates transcription. J Biol Chem. 2004; 279:1867–71. [PubMed: 14660634]
- 16. Ye Y, Scheel H, Hofmann K, Komander D. Dissection of USP catalytic domains reveals five common insertion points. Mol Biosyst. 2009; 5:1797–808. [PubMed: 19734957]
- 17. Lee KK, Florens L, Swanson SK, Washburn MP, Workman JL. The deubiquitylation activity of Ubp8 is dependent upon Sgf11 and its association with the SAGA complex. Mol Cell Biol. 2005; 25:1173–82. [PubMed: 15657442]
- Kohler A, Zimmerman E, Schneider M, Hurt E, Zheng N. Structural basis for assembly and activation of the heterotetrameric SAGA histone H2B deubiquitinase module. Cell. 2010; 141:606–17. [PubMed: 20434206]
- Samara NL, Datta AB, Berndsen CE, Zhang X, Yao T, Cohen RE, et al. Structural insights into the assembly and function of the SAGA deubiquitinating module. Science. 2010; 328:1025–9.
 [PubMed: 20395473]
- 20. Samara NL, Ringel AE, Wolberger C. A role for intersubunit interactions in maintaining SAGA deubiquitinating module structure and activity. Structure. 2012; 20:1414–24. [PubMed: 22771212]
- Avvakumov GV, Walker JR, Xue S, Finerty PJ Jr, Mackenzie F, Newman EM, et al. Aminoterminal dimerization, NRDP1-rhodanese interaction, and inhibited catalytic domain conformation of the ubiquitin-specific protease 8 (USP8). J Biol Chem. 2006; 281:38061–70. [PubMed: 17035239]
- 22. Hu M, Li P, Li M, Li W, Yao T, WUJW, et al. Crystal structure of a UBP-family deubiquitinating enzyme in isolation and in complex with ubiquitin aldehyde. Cell. 2002:111.

 Faesen AC, Dirac AM, Shanmugham A, et al. Mechanism of USP7/HAUSP activation by its C-terminal ubiquitin-like domain and allosteric regulation by GMP-synthetase. Mol Cell. 2011; 44:147–59. [PubMed: 21981925]

- 24. Dang LC, Melandri FD, Stein RL. Kinetic and mechanistic studies on the hydrolysis of ubiquitin C-terminal 7-amido-4-methylcoumarin by deubiquitinating enzymes. Biochemistry. 1998; 37:1868–79. [PubMed: 9485312]
- 25. Phillips K, de la Pena AH. The combined use of the Thermofluor assay and ThermoQ analytical software for the determination of protein stability and buffer optimization as an aid in protein crystallization. Curr Protoc Mol Biol. 2011; Chapter 10(Unit 10):28. [PubMed: 21472694]
- 26. Ventii KH, Wilkinson KD. Protein partners of deubiquitinating enzymes. Biochem J. 2008:414.
- 27. Wolberger C. Mechanisms for regulating deubiquitinating enzymes. Protein Sci. 2014; 23:344–53. [PubMed: 24403057]
- 28. Reyes-Turcu FE, Wilkinson KD. Polyubiquitin binding and disassembly by deubiquitinating enzymes. Chem Rev. 2009; 109:1495–508. [PubMed: 19243136]
- 29. Leggett D, Hanna J, Borodovsky A, Crosas B, et al. Multiple associated proteins regulate proteasome structure and function. Molecular Cell. 2002; 10:495–507. [PubMed: 12408819]
- 30. Verma R, Aravind L, Oania R, Mcdonald WH, et al. Role of Rpn11 metalloprotease in deubiquitination and degradation by the 26S proteasome. Science. 2002; 298:611–615. [PubMed: 12183636]
- 31. Yao T, Song L, Xu W, Demartino GN, et al. Proteasome recruitment and activation of the Uch37 deubiquitinating enzyme by Adrm1. Nat Cell Biol. 2006; 8:994–1002. [PubMed: 16906146]
- 32. Kee Y, Yang K, Cohn MA, Haas W, Gygi SP, D'Andrea AD. WDR20 regulates activity of the USP12 x UAF1 deubiquitinating enzyme complex. J Biol Chem. 2010; 285:11252–7. [PubMed: 20147737]
- 33. Cohn MA, Kee Y, Haas W, Gygi SP, D'Andrea AD. UAF1 is a subunit of multiple deubiquitinating enzyme complexes. J Biol Chem. 2009; 284:5343–51. [PubMed: 19075014]
- 34. Cohn MA, Kowal P, Yang K, Haas W, Huang TT, Gygi SP, et al. A UAF1-containing multisubunit protein complex regulates the Fanconi anemia pathway. Mol Cell. 2007; 28:786–97. [PubMed: 18082604]
- 35. Scheuermann JC, de Ayala Alonso AG, Oktaba K, Ly-Hartig N, McGinty RK, Fraterman S, et al. Histone H2A deubiquitinase activity of the Polycomb repressive complex PR-DUB. Nature. 2010; 465:243–7. [PubMed: 20436459]
- 36. Zhao Y, Lang G, Ito S, et al. A TFTC/STAGA module mediates histone H2A and H2B deubiquitination, coactivates nuclear receptors, and counteracts heterochromatin silencing. Mol Cell. 2008; 29:92–101. [PubMed: 18206972]
- Zhang XY, Varthi M, Skyes SM, et al. The putative cancer stem cell marker USP22 is a subunit of the human SAGA complex required for activated transcription and cell-cycle progession. Mol Cell. 2008; 29:102–11. [PubMed: 18206973]
- 38. Lang G, Bonnet J, Umlauf D, et al. The tightly controlled deubiquitination activity of the human SAGA complex differentially modifies distinct gene regulatory elements. Mol Cell Biol. 2011; 31:3734–44. [PubMed: 21746879]
- 39. Zhang XY, Pfeiffer HK, Thorne AW, et al. USP22, an hSAGA subunit and potential cancer stem cell marker, reverses the polycomb-catalyzed ubiquitylation of histone H2A. Cell Cycle. 2008; 7:1522–4. [PubMed: 18469533]
- 40. Liu YL, Yang YM, Xu H, et al. Aberrant expression of USP22 is associated with liver metastasis and poor prognosis of colorectal cancer. J Surg Oncol. 2011; 103:283–9. [PubMed: 21337558]
- 41. Yang M, Liu YD, Wang YY, et al. Ubiquitin-specific protease 22: a novel molecular biomarker in cervical cancer prognosis and therapeutics. Tumour Biol. 2014; 35:929–934. [PubMed: 23979981]
- Prenzel T, Nahrmann YB, Kramer F, et al. Estrogen-Dependent gene transcription in human breast cancer cells relies upon proteasome-dependent monoubiquitination of histone H2B. Cancer Research. 2011; 71:5739–53. [PubMed: 21862633]
- 43. Hahn MA, Dickson KA, Jackson S, et al. The tumor suppressor CDC73 interacts with the ring finger proteins RNF20 and RNF40 and is required for the maintenance of histone 2B monoubiquitination. Human Mol Genetics. 2012; 21:559–568.

44. Komander D, Clague MJ, Urbe S. Breaking the chains: structure and function of the deubiquitinase. Nat Rev Mol Cell Biol. 2009; 10:550–63. [PubMed: 19626045]

- 45. Adams PD, Grosse-Kunstleve RW, Hung LW, Ioerger TR, McCoy AJ, Moriarty NW, et al. PHENIX: building new software for automated crystallographic structure determination. Acta crystallographica Section D, Biological crystallography. 2002; 58:1948–54.
- 46. Murshudov G, Vagin A, Dodson E. Refinement of marcomolecular structures by the maximum likelihood method. Acta crystallographica Section D. 1997; 53:240–255.
- 47. Emsley P, Lohkamp B, Scott WG, Cowtan K. Features and development of Coot. Acta crystallographica Section D, Biological crystallography. 2010; 66:486–501.

Highlights

• The Sgf73 subunit of the SAGA deubiquitinating module (DUBm) activates the catalytic Ubp8 subunit.

- The mechanism by which Sgf73 contributes to deubiquitinating activity is unknown.
- Sgf73 mutations at the interface with Ubp8 decrease DUBm activity.
- Sgf73 maintains DUBm stability and structure of the Ubp8 ubiquitin-binding pocket.

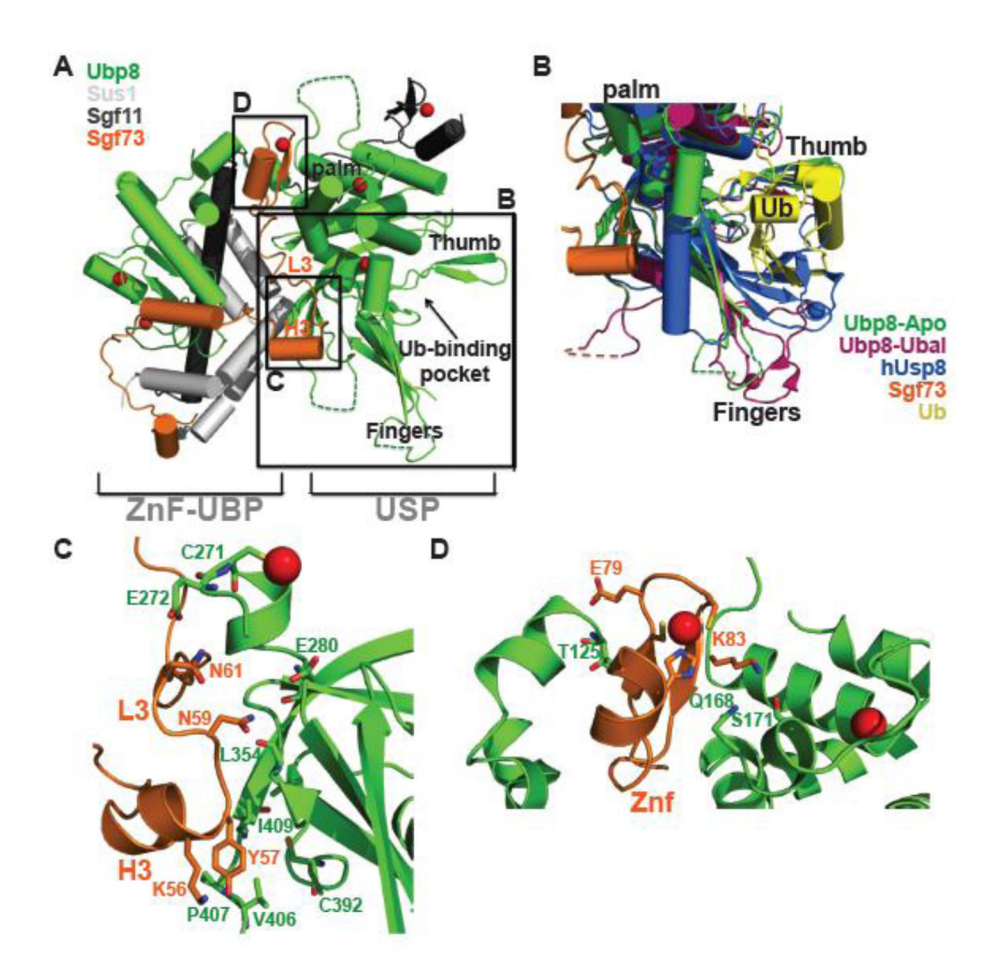
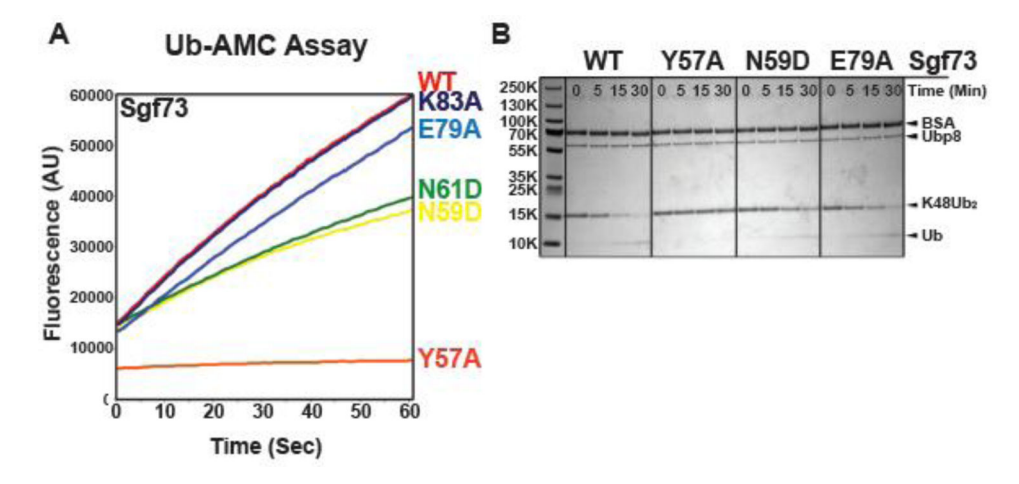


Fig 1. Sgf73 mediates interactions between two lobes of SAGA DUB module

(A) Overall view of the yeast SAGA DUB module. Ubp8 (green), Sus1 (light gray), Sgf11 (dark gray) and Sgf73 (orange) are shown in cartoon representation with disordered residues depicted as dashed lines. Zinc ions are shown as red spheres. The fingers, palm and thumb sub-domains of the Ubp8 USP domain are labeled. Letters next to solid boxes surrounding the ubiquitin -binding region of Ubp8 and two interfaces between Ubp8 and Sgf73 provide the key to figure panels showing further detail on the interactions. (B) Superposition of the ubiquitin-binding region in Ubp8-Apoenzyme (DUBm-Apo), Ubp8-ubiquitin aldehyde (DUBm-Ubal) and hUsp8. Ubp8-Apo (green), Ubp8-Ubal (magenta), hUsp8 (blue), Sgf73 (orange) and Ub (yellow) are shown in cartoon representation with disordered residues depicted as dashed lines. (C) The H3-L3 region of Sgf73 (orange) docks on the back (buried) side of the fingers region of Ubp8 (green). (D) The Sgf73-ZnF (orange) is wedged between the two domains of Ubp8 (green).



 $Fig\ 2.\ Sgf73\ mutations\ abutting\ Ubp8\ Ub-binding\ region\ decrease\ deubiquitinating\ activity\ of\ the\ DUB\ module$

(A) Ub-AMC hydrolysis time course showing activity of wild type and mutant DUBm complexes. (B) Gel assay of K48-linked diubiquitin cleavage by DUB module containing wild-type and Sgf73 mutants. Gel stained with Coomassie. All experiments were performed at 30° C.

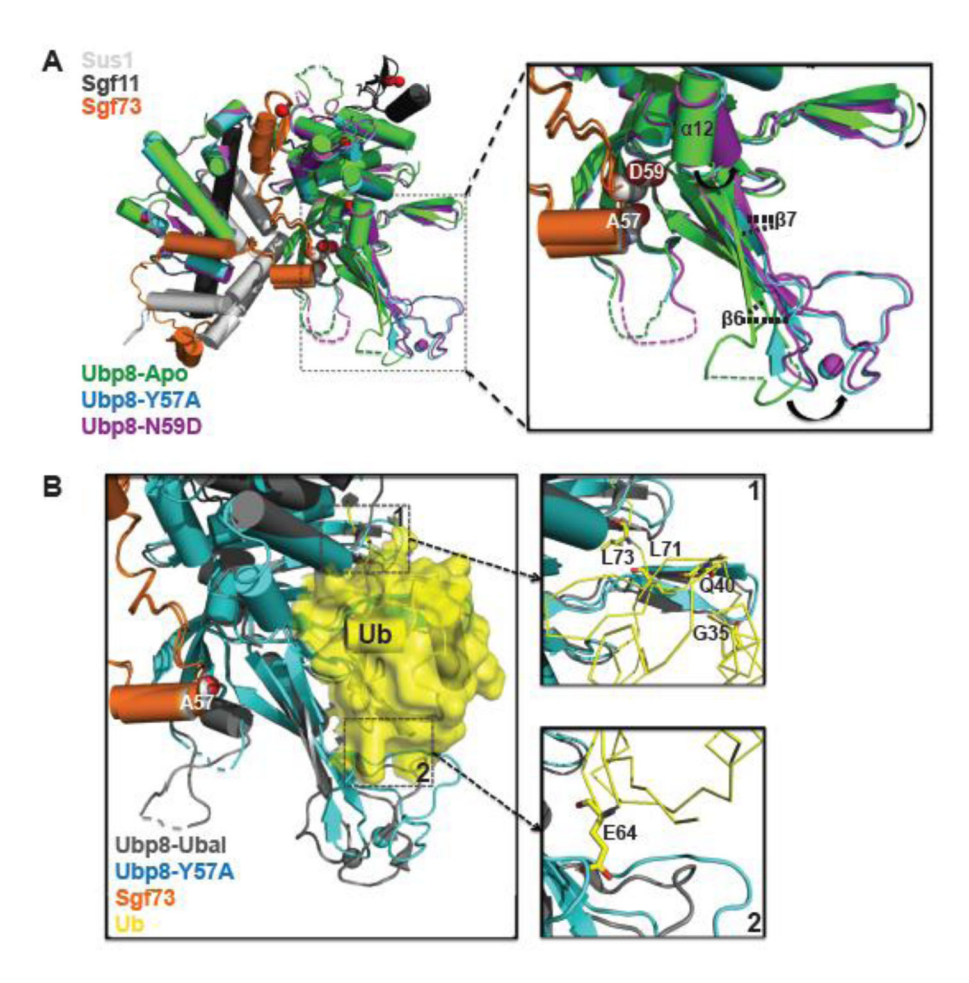


Fig 3. Effects of Sgf73 mutants on DUB module structure

(A) Superposition of DUBm-WT, DUBm-Sgf73 Y57A and DUBm-Sgf73 N59D . Ubp8-Apo (green), Ubp8-Y57A (cyan) and Ubp8-N59D (magenta) are shown in cartoon representation. Solid box shows a close-up view of the Ub-binding region of Ubp8. Black arrows show where conformational changes occur in the Ubp8 fingers region of DUBm-Sgf73 Y57A . The α helix α 12 and β strands β 6 and β 7 are labeled. (B) Steric clashes between Ubp8 and bound ubiquitin caused by the Sgf73 Y57A mutation. Superposition of Ubp8 Ubbinding regions from DUBm-Ubal (gray) and DUBm-Sgf73 Y57A (cyan) shows two possible steric clashes between Ubp8-Y57A and ubiquitin. Right upper box: close-up view of clash 1. Side chains of Ubiquitin G35, Q40, L71 and L73 clash with the thumb region of Ubp8-Y57A. Right bottom box: close-up view of clash 2. Side chain of ubiquitin E64 clashes with the loop of Ubp8-Y57A. All highlighted residues are shown in stick representation.

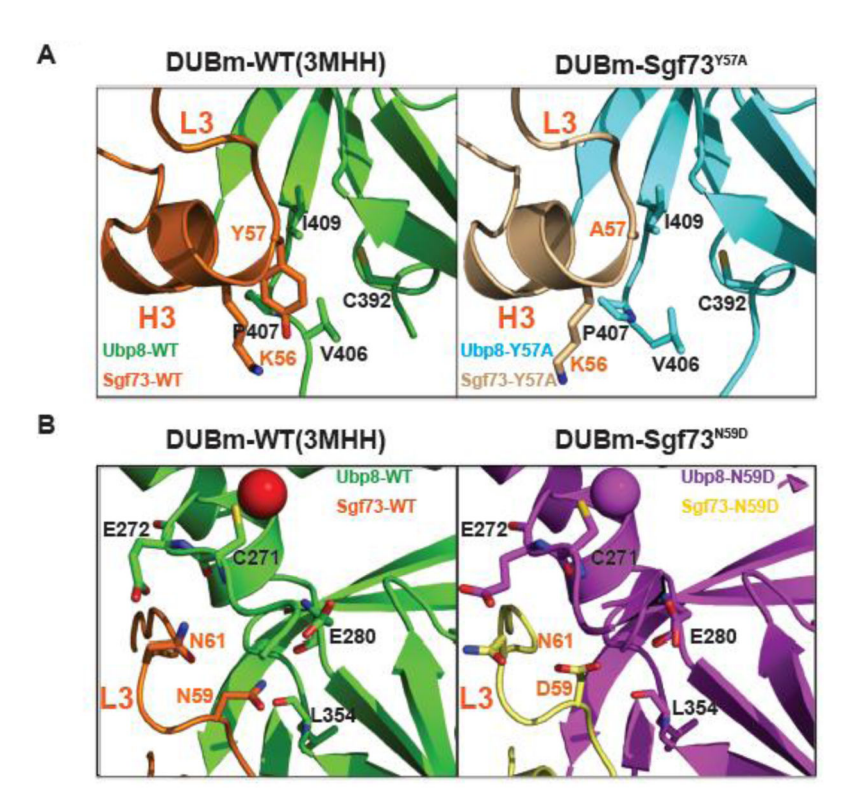


Fig 4. Sgf73 mutations disrupt interactions between Sgf73 H3-L3 region and Ubp8 USP domain (A) Structural comparison between DUBm-WT and DUBm-Sgf73^{Y57A}. Left: hydrophobic interactions between Sgf73 H3 region and Ubp8 USP domain. Right: same set of hydrophobic interactions is disrupted in DUBm-Sgf73^{Y57A}. (B) Comparison of DUBm-WT and DUBm-Sgf73^{N59D} structures. Left: Hydrogen bonds and charge-charge interactions between Sgf73 L3 region and Ubp8 USP domain. Right: most of interactions shown in left panel are disrupted in DUBm-Sgf73^{N59D}. Zinc ions are shown as spheres.

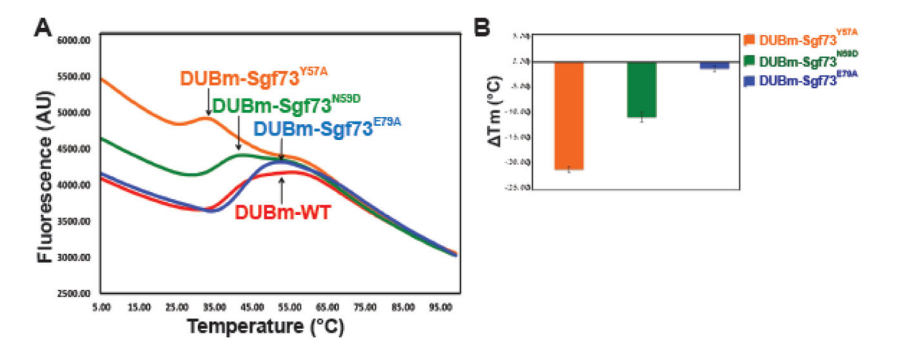


Fig 5. Sgf73 mutations reduce the stability of DUB module

Results of thermal shift assays of wild-type and mutant DUBm stability. (A) Melting curves of DUBm-WT (red), DUBm-Sgf73 Y57A (orange), DUBm-Sgf73 N59D (green) and DUBm-Sgf73 E79A (blue). (B) Changes in the melting temperature ($\,T_m$) between DUBm-WT and Sgf73 mutants. The bars represent the median $\,T_m$ values. A negative median $\,T_m$ value signifies that the mutant reduces the stability of the DUB module.

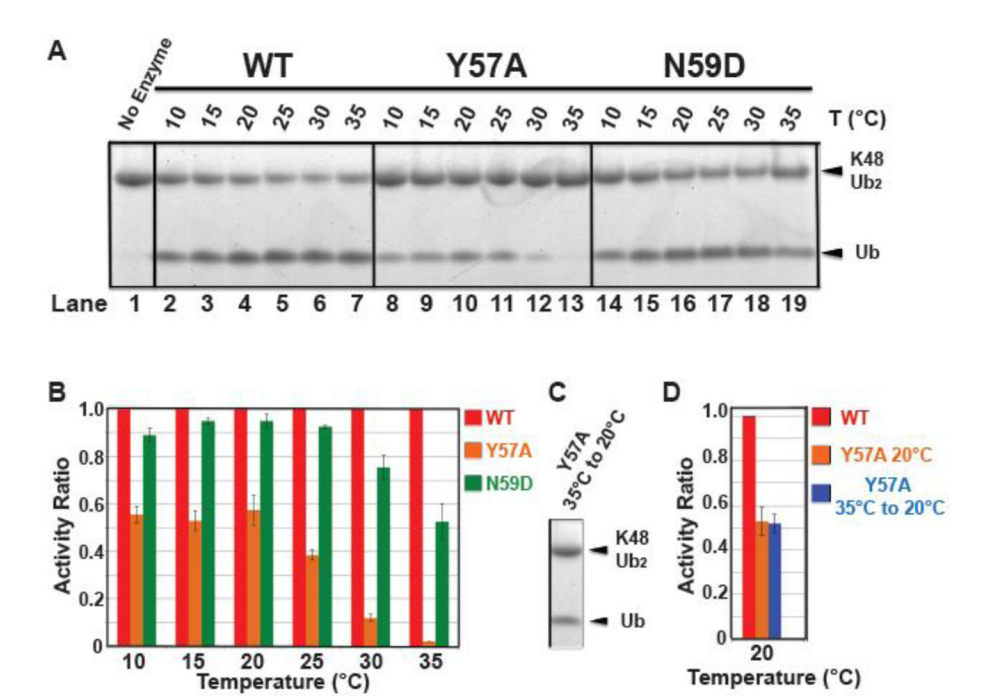


Fig 6. The deubiquitinating activity of DUBm-Sgf73^{Y57A} is temperature sensitive (A) Gel assay showing cleavage of fluorescein-labeled K48 diubiquitin by wild-type and Sgf73 mutants at temperatures ranging from 10°C to 35°C. The experiments were done in triplicate and gel images were recorded using a Typhoon Variable Mode Imager monitoring fluorescence. (B) DUB activity of Sgf73 mutants is temperature sensitive (Bar graph depiction of (A)). The DUB activity of DUBm-WT was normalized to 1 at individual temperature. The DUB activities of Sgf73 mutants were calculated as the ratio value compared to that of DUBm-WT at the same temperature. The bars represent the median ratio values. (C) The DUB activity of DUBm Sgf73^{Y57A} is reversible in certain temperature range. DUBm-Sgf73^{Y57A} was incubated at 35°C for 10 minutes before performing the same assay as (A) at 20°C. (D) The DUB activity of DUBm-Sgf73^{Y57A} shown in (C) was normalized and compared to both the DUB activities of DUBm-WT and DUBm-Sgf73^{Y57A} shown in (A). The bars represent the median ratio values.

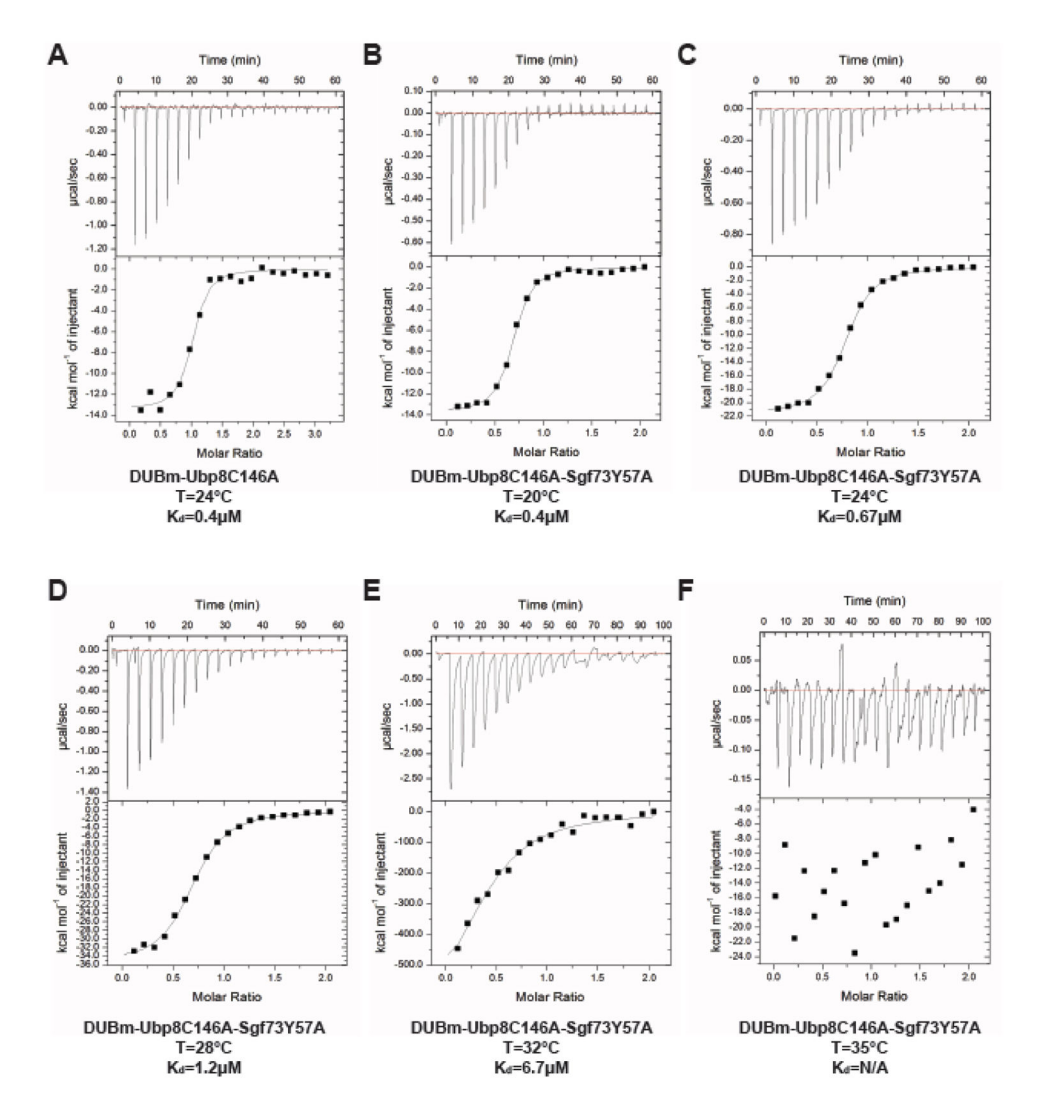


Fig 7. Temperature sensitivity of DUBm-Ubp8^{C146A}-Sgf73^{Y57A} binding to diubiquitin (A) Isothermal Titration Calorimetry (ITC) measurements of the interaction between DUBm-Ubp8^{C146A} and K48-linked diubiquitin performed at 24°C. Experimental details are provided in *Materials and Methods*. (B–F) ITC measurements for binding of DUBm-Ubp8^{C146A}-Sgf73^{Y57A} to K48-linked diubiquitin performed at 20°C, 24°C, 28°C, 32°C and 35°C, respectively. The same amount of DUBm-Ubp8^{C146A}-Sgf73^{Y57A} and K48-linked diubiquitin were used for each measurement.

Yan and Wolberger Page 24

Table 1

X-Ray Crystallography Data and Refinement Statistics

Data Collection Statistics	DUBm-Sgf73 ^{Y57A}	DUBm-Sgf73 ^{N59D}				
Energy (keV)	12	12				
Resolution (Å)	2.80	2.36				
Unique reflections	34987	59279				
Redundancy	3.8(3.7)	3.8(3.6)				
Completeness (%)	99.78(99.7)	100(99.6)				
Average I/σ (I)	23.2(2.14)	23(1.68)				
R _{sym} (%)	8.5	8.3				
Refinement Statistics						
Space Group and	P2 ₁	P2 ₁				
Unit Cell (Å)	a=80.7 b=67.3 c=137.1	a=81 b=68 c=137.8				
Molecules per asymmetric unit	2	2				
R _{work} (%)	17.6	18.3				
R _{free} (%)	25.5	24.4				
Rmsd bonds (Å)	0.011	0.009				
Rmsd angles (o)	1.211	1.228				
Protein atoms	10617	11236				
Water molecules	52	183				
Zinc (II) ions	13	16				
Average B (Å ²)	51.258	36.0				
Ramachandran plot						
Favored (%)	96	96				
Allowed (%)	4	4				
Disallowed (%)	0	0				

Rmsd, root-mean-square-deviation

Yan and Wolberger Page 25

 Table 2

 Summary of thermodynamic parameters obtained from the ITC measurements shown in Figure 7

#	Complex	$Temperature \ (^{\circ}C)$	Number of binding sites (N)	Dissociation constant (Kd, µM)
A	$DUBm\text{-}Ubp8^{C146A} + K48\text{-}Ub_2$	24	1	0.4±0.1
В	$DUBm\text{-}Ubp8^{C146A}\text{-}~Sgf73^{Y57A} + K48\text{-}Ub_2$	20	0.7	0.4 ± 0.04
C	$DUBm\text{-}Ubp8^{C146A}\text{-}~Sgf73^{Y57A} + K48\text{-}Ub_2$	24	0.7	0.67 ± 0.04
D	$DUBm\text{-}Ubp8^{C146A}\text{-}~Sgf73^{Y57A} + K48\text{-}Ub_2$	28	0.7	1.2±0.1
E	$DUBm\text{-}Ubp8^{C146A}\text{-}~Sgf73^{Y57A}\text{+}K48\text{-}Ub_2$	32	0.4	6.7±1.5
F	$DUBm\text{-}Ubp8^{C146A}\text{-}~Sgf73^{Y57A} + K48\text{-}Ub_2$	35	N/A	N/A